

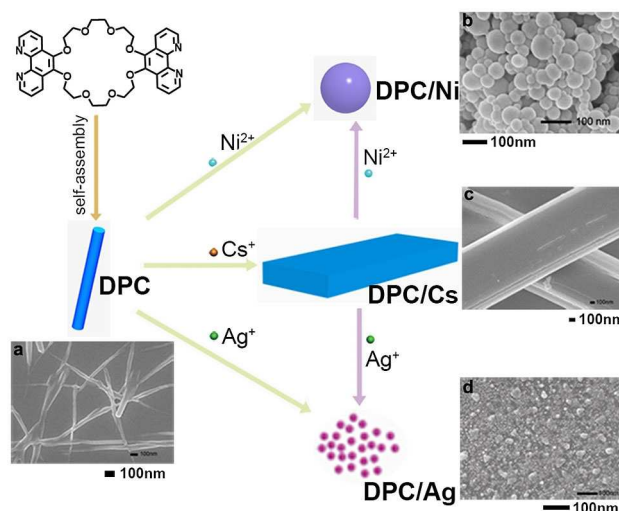
# Tunable Supramolecular Nanoarchitectures Constructed by the Complexation of Diphenanthro-24-Crown-8/Cesium(I) with Nickel(II) and Silver(I) Ions

Zhi-Yuan Zhang,<sup>[a]</sup> Yong Chen,<sup>[a]</sup> Yan Zhou,<sup>[a]</sup> and Yu Liu<sup>\*[a, b]</sup>

Tunable supramolecular nanoarchitectures have received enormous attention because of their potential in materials fabrication. Herein, a variety of morphologically intriguing nanoarchitectures have been constructed from diphenanthro-24-crown-8 ether (DPC) and metal ions. SEM and TEM showed that the self-assembled nanofibers undergo a Cs<sup>+</sup>-induced transformation into regular nanoribbons, and further into nanospheres and nanoparticles by the complexation of Ni<sup>II</sup> and Ag<sup>I</sup> ions because of the strong ion-dipole interaction. Moreover, the X-ray crystal structure determination and powder X-diffraction data further confirmed that these morphological transformations resulted from the different complexation between DPC and metal ions. This result provides a new strategy for the subtle manipulation of supramolecular assemblies.

Self-assembly is the compromise of various noncovalent bonding interactions, such as ion-ion interactions, ion-dipole interactions, hydrogen bonding,  $\pi$ - $\pi$  interactions, Van der Waals Forces and so on. When designing a supramolecular system, it is crucial to take into account the interplay of all of these interactions comprehensively. However, in most cases, the inherent unmeasurable nature of the interactions makes the construction and regulation of assembly an elusive goal. Some excellent works have been reported in the past years.<sup>[1]</sup> Recently, the modulation of assembled structures from one morphology to another by redox,<sup>[2]</sup> heat<sup>[3]</sup> and light<sup>[4]</sup> was achieved. We previously reported photocontrolled reversible conversion of assemblies by the trans/cis isomerization of azobenzene and a variety of tunable morphologically interesting aggregates constructed by host-guest complexation.<sup>[5]</sup>

Motivated by our ongoing interest on the morphologically conversion of nanosupramolecular assemblies and potential application in material manufacturing, herein we report a diphenanthro-24-crown-8 (DPC) which can be regulated from nanofibers to regular nanoribbons and then to nanospheres



**Scheme 1.** Schematic illustration of tunable nanostructures and SEM micrographs of assemblies. (a) DPC (nanofibers), (b) DPC/Ni (nanospheres), (c) DPC/Cs (nanoribbons) and (d) DPC/Ag (nanoparticles).

and nanoparticles by different metals (Scheme 1). A key to achieve this multilevel manipulation was the accurate utilizing of four different noncovalent forces provided by DPC and ethanol: the  $\pi$ - $\pi$  stacking of 1,10-phenanthroline group, the ion-dipole interactions of crown ether motif with alkalis, the coordination interactions of 1,10-phenanthroline with transition metals and the H-bond between DPC and ethanol. The crystal uncovered the multiple H-bonding between DPC and ethanol, which were vital to the morphological transformation.

As  $\pi$ -stacking of phenanthroline derivatives and the binding character of 24-crown-8 for Cs<sup>+</sup> had been well established,<sup>[6]</sup> it was possible for DPC to form nanostructures by self-assembly and change its morphology by complexation with Cs<sup>+</sup>. As anticipated, self-assembly DPC did yield fiber-like structures after the evaporation of solvent (Scheme 1, Figure 1a,b). The addition of CsCl produced large size nanoribbon DPC/Cs (Scheme 1, Figure 1e,f). As a typical example, a mixture of DPC (10 mM) and CsCl (10 mM) was allowed to stand at 25 °C in ethanol (EtOH). 6  $\mu$ L of the reaction mixture was subjected to scanning electron microscopy (SEM) after air-dried. As shown in Figure 1e,f, nanoribbons with a length of 50 to 400  $\mu$ m and width of 0.2 to 3  $\mu$ m were observed. The size matched well with transmission electron microscopy (TEM) images (Figure S1c,d). TEM-element mapping pattern verified the uniform distribution of Cs<sup>+</sup> in nanoribbon. The clear border indicated that the Cs<sup>+</sup> was participated in the construction of assembly but not

[a] Z.-Y. Zhang, Dr. Y. Chen, Dr. Y. Zhou, Prof. Dr. Y. Liu  
Department of Chemistry  
State Key Laboratory of Elemento-Organic Chemistry  
Nankai University, Tianjin 300071 (P. R. China)  
E-mail: yuliu@nankai.edu.cn

[b] Prof. Dr. Y. Liu  
Collaborative Innovation Center of Chemical Science  
and Engineering (Tianjin)  
Nankai University, Tianjin 300071 (P. R. China)

Supporting information for this article is available on the WWW under <https://doi.org/10.1002/cplu.201900002>

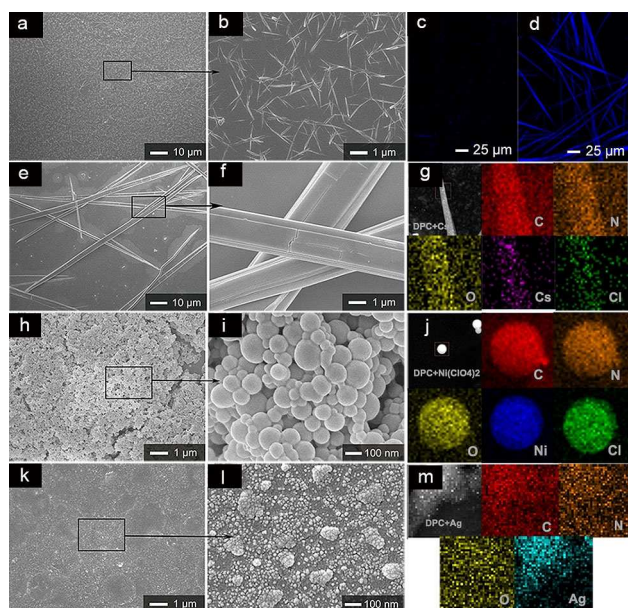


**Figure 1.** (a, b, e, f, h, i, k, l) SEM images, (g, j, m) element mapping pattern and (c, d) LCSM micrographs of air-dried EtOH/water dispersions of (a, b, c) DPC, (d, e, f, g) DPC/Cs, (h, i, j) DPC/Ni, and (k, l, m) DPC/Ag ([DPC] = [CsCl] = [Ni(ClO<sub>4</sub>)<sub>2</sub>] = [AgNO<sub>3</sub>] = 10 mM in EtOH).

absorbed in the surface (Figure 1g). The untapped coordination ability of phenanthroline inspired us to explore more various transformation of morphology. Interestingly, when titration DPC with Ni(ClO<sub>4</sub>)<sub>2</sub>, aggregated nanospheres DPC/Ni appeared (Figure 1h,i and Figure S1e,f). The diameter of nanospheres was ranging from 50 to 100 nm. TEM-element mapping pattern clearly validated the existence of Ni<sup>2+</sup> in the nanosphere (Figure 1j). In the case of AgNO<sub>3</sub>, much smaller assembly DPC/Ag in the morphology of nanoparticles appeared with the diameter of 10 nm to 20 nm (Figure 1k,l and Figure S1g,h). The strong elemental signal of Ag proved its involvement in the assembly (Figure 1m).

The binding modes between DPC and three metals were investigated by UV/Vis, fluorescence, <sup>1</sup>H NMR and mass spectrometry. Neither absorption nor fluorescence spectra displayed any change upon the titration of CsCl which indicated that the Cs<sup>+</sup> did not bind with the phenanthroline moieties and possibly located in the crown ether group (Figure 2a,b). This anticipation was confirmed by <sup>1</sup>H NMR. The protons of phenanthroline at 7.7, 8.7 and 9.0 ppm exhibited no change but crown ether protons at 3.7, 3.9 and 4.4 ppm shifted slightly upon the addition of CsCl (Figure S2). This is reasonable as crown ether have a remarkable binding ability for alkali metal ions and the cavity radius and donor group orientation in 24-crown-8 is most favourable for Cs<sup>+</sup>.<sup>[7]</sup> Matrix-assisted laser desorption/ionization-time-of-flight mass spectrometry (MALDI-TOF-MS) confirmed the 1:1 complex DPC/Cs<sup>+</sup> (m/z 785.164, calcd value 785.159 for [M]<sup>+</sup>, Figure S3). However, the absorption band centred at 232 nm and 272 nm decreased dramatically upon titration with Ni(ClO<sub>4</sub>)<sub>2</sub> which indicated the binding of phenanthroline with metals.<sup>[8]</sup> The immensely attenuation of fluorescence intensity at 450 nm further confirmed the binding

of phenanthroline with Ni<sup>2+</sup> (Figure 2d). The binding constant (K<sub>s</sub>) was determined as 1.80 × 10<sup>8</sup> M<sup>-1</sup> (Figure S6a,b). Besides, the complete disappearance of phenanthroline and crown ether protons indicated the formation of DPC/Ni complex which had poor solubility (Figure S2). As the liganacy of Ni<sup>2+</sup> was changeable,<sup>[9]</sup> we validated complex stoichiometry by Job's plot (Figure S4). The dependence of the absorbance at 262 nm toward Ni<sup>2+</sup> concentration determined complex stoichiometry as 1:1 or n:n, considering the <sup>1</sup>H NMR data discussed above, n:n was more reasonable. In the case of AgNO<sub>3</sub>, the absorption band centred at 232 nm and 272 nm were sharply weakened by AgNO<sub>3</sub> (Figure 2e). The emission also quenched which could be attributed to the heavy atom effect of Ag<sup>+</sup> (Figure 2f). The binding constant (K<sub>s</sub>) was determined as 7.87 × 10<sup>6</sup> M<sup>-1</sup> (Figure S6c,d).<sup>[10]</sup> <sup>1</sup>H NMR gave weakened and broaden signal (Figure S2). All these data indicated that DPC bound with Ag<sup>+</sup> in the phenanthroline motif. Job's plot confirmed complex stoichiometry as 1:1 or n:n (Figure S5). As 2:1 coordination mode of phenanthroline derivatives with Ni<sup>2+</sup> and Ag<sup>+</sup> has been well established,<sup>[11,12]</sup> we proposed that every two phenanthroline motifs of DPC coordinated with one Ni<sup>2+</sup> or Ag<sup>+</sup>. Therefore, liner oligomer formed and further entangled into nanospheres (DPC/Ni) or nanoparticles (DPC/Ag) (Figure 3d). A reasonable assembly mode was illustrated in Figure 3d. The DPC/Cs adopted the V-shaped stacking, while Cs<sup>+</sup> located on the cavity of crown ether. For DPC/Ni, the Ni<sup>2+</sup> connected DPC to form a linear structure which further entwined into large nanosphere. This mode was also applicable to DPC/Ag.

Inspired by above transformation of morphology and the different anchoring points of DPC, we hypothesized that further manipulation was probably available if Ni<sup>2+</sup> or Ag<sup>+</sup> were introduced to the DPC/Cs system. The disappearance and broadening of <sup>1</sup>H NMR signal proved the formation of DPC/Ni or DPC/Ag upon the addition of Ni(ClO<sub>4</sub>)<sub>2</sub> or AgNO<sub>3</sub> to DPC/Cs system (Figure S7). The detailed morphological conversion was recorded by TEM (Figure S9). In the case of Ni<sup>2+</sup>, one equivalents of Ni(ClO<sub>4</sub>)<sub>2</sub> was added to the DPC/Cs system (10 mM), after shaking for 1 minute, 6 μL of the reaction mixture was subjected to TEM after air-dried. Interestingly, nanospheres same as DPC/Ni were observed and the conversion process were captured by TEM. In Figure S9, the remained ribbon-like DPC/Cs assembly were surrounded by the newly formed spherical assembly DPC/Ni. The spherical nanostructures mainly formed in the border of nanoribbon and the centre of which was halted on the way of transformation by the evaporation of solvent. In the remote region, dispersive spheres in the same size and morphology with DPC/Ni assembly were completely transformed (Figure S9d). All these images promoted us to propose that the attacking of Ni<sup>2+</sup> to nanoribbons most probably started from the external by the strong ion-dipole force between phenanthroline and Ni<sup>2+</sup>. The short reaction time (1 min) and fast evaporation of solvent ensured the capturing of the conversion. Enough time made the nanoribbons transformed into nanospheres completely (Figure S8). TEM-element mapping pattern validated the existence of Ni<sup>2+</sup> and Cs<sup>+</sup> in the nanospheres which indicated that the

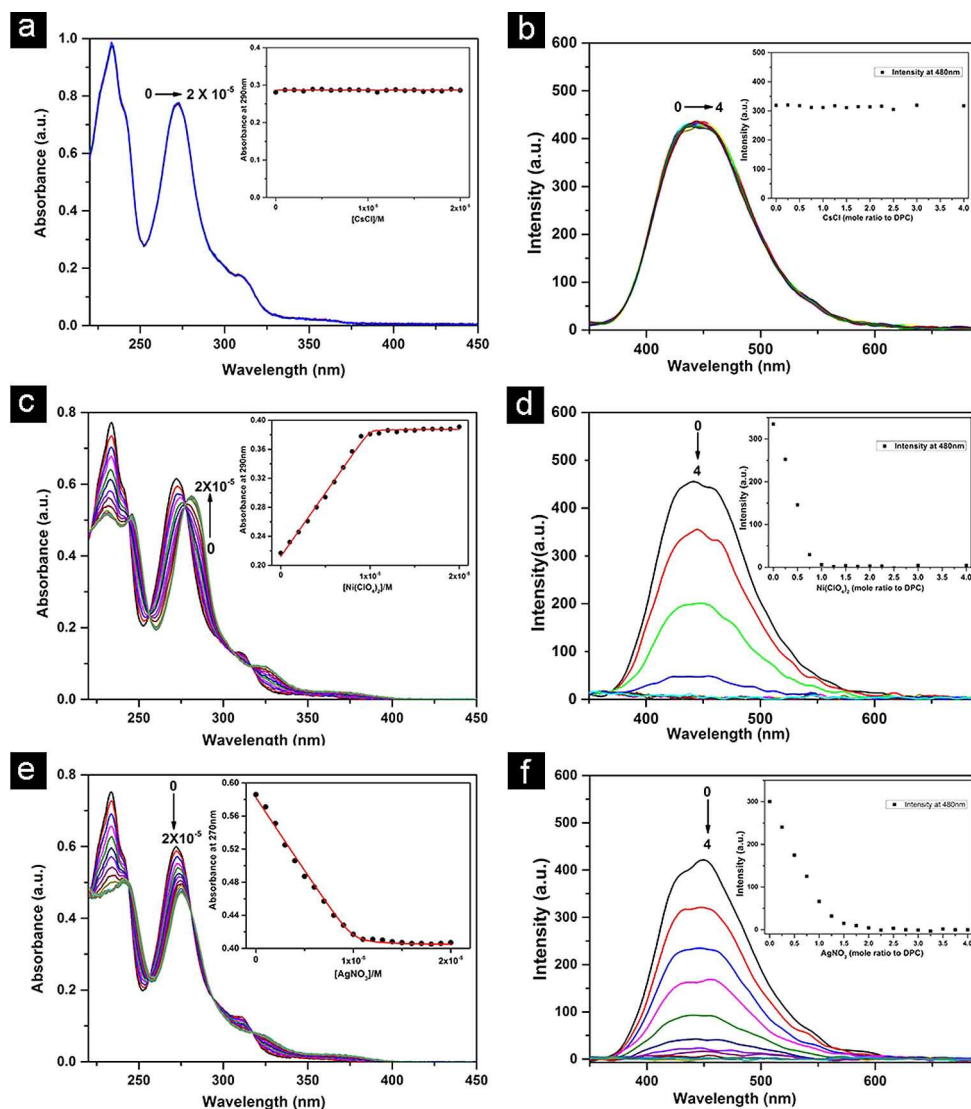


**Figure 2.** (a, c, e) UV/Vis spectra of DPC upon titration with metals and (inset) absorption changes at certain wavelengths upon titration with (a) CsCl, (c) Ni(ClO<sub>4</sub>)<sub>2</sub>, (e) AgNO<sub>3</sub> ([DPC] = 0.01 mM in ethanol, [CsCl] = [Ni(ClO<sub>4</sub>)<sub>2</sub>] = [AgNO<sub>3</sub>] changed from 0 to 0.02 mM); (b, d, f) fluorescence spectra of DPC upon titration with metals and (inset) fluorescence intensity changes at 480 nm upon titration with (b) CsCl, (d) Ni(ClO<sub>4</sub>)<sub>2</sub>, (f) AgNO<sub>3</sub> ([DPC] = 0.01 mM in ethanol, CsCl, Ni(ClO<sub>4</sub>)<sub>2</sub>, AgNO<sub>3</sub> mole ratio to constituent DPC changed from 0 to 400 %).

transformation was originated from the bonding of Ni<sup>2+</sup> (Figure S10). For Ag<sup>+</sup>, we chose CsNO<sub>3</sub> but not original CsCl as to avoid the mischief of Cl<sup>-</sup> to Ag<sup>+</sup>. There was no doubt that the replacement of counter ion nearly had no effect on the assembly as the complex had same morphology and characteristic reflection of powder X-ray diffraction (XRD) with that of CsCl (Figures S11 and S12). The titration of AgNO<sub>3</sub> resulted in the gradually decrease of DPC/Cs and the formation of nanoparticles (Figure S13). The completely transformation resulted in the formation of the nanoparticles (Figure S13). The ribbon in the widths of 480 nm was transforming into nanoparticles (Figure S14a), the conversion occurred at both the end and the middle part of the nanoribbon (Figure S14c). These figures revealed that the Ag<sup>+</sup> possibly adopted the same offensive pattern as Ni<sup>2+</sup>. TEM-element mapping pattern proved the existence of Ag<sup>+</sup> and Cs<sup>+</sup> in the nanoparticles (Figure S15).

Thus, the second level manipulation triumphantly accomplished by the morphological transformation from nanoribbons to nanospheres and nanoparticles.

Due to the fluorescence characteristics and large size of these assemblies, we further studied the assemblies and multi-level morphological manipulation by Laser Confocal Scanning Microscope (LCSM). The fluorescence reserved for DPC and DPC/Cs and disappeared for DPC/Ni and DPC/Ag after the vapping of solvent, which fitted well with the photophysical properties in solution (Figure 1c,d and Figure S16). When Ni(ClO<sub>4</sub>)<sub>2</sub> or AgNO<sub>3</sub> was added to DPC/Cs system, the fluorescence absolutely disappeared (Figures S17 and S18).

The assembly mode of DPC and DPC/Cs were still unaddressed so far, fortunately, the single crystal of DPC and XRD provided detailed information (Figure 3a,b). The CCDC number is 1884016. DPC crystal belonging to the monoclinic

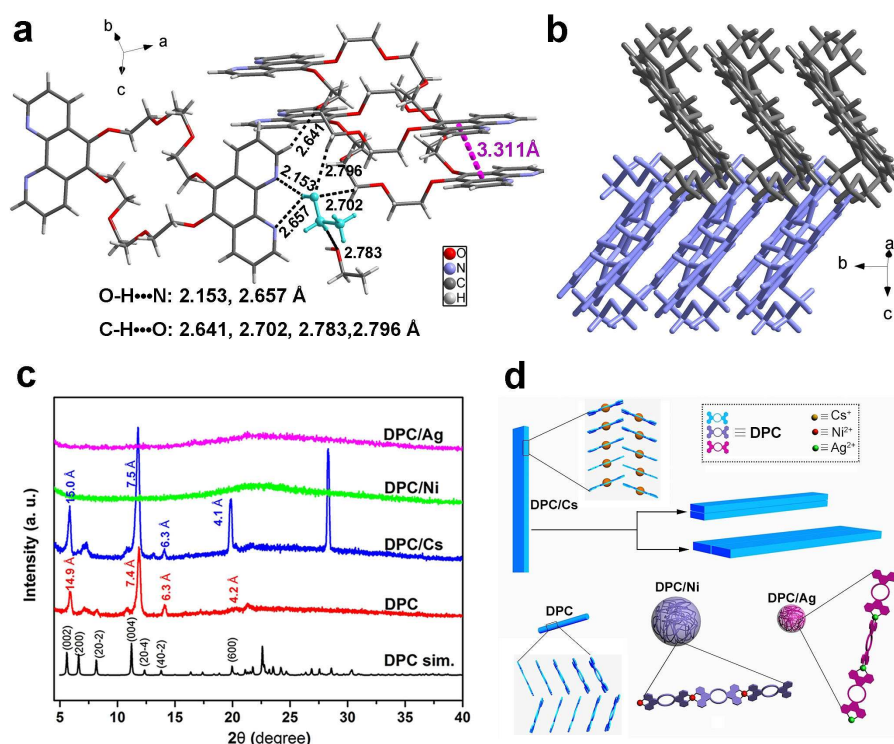


**Figure 3.** (a, b) X-ray single-crystal diffraction of DPC (the ethanol was in cyan), (c) XRD patterns of the DPC/Ag, DPC/Ni, DPC/Cs, DPC, simulated XRD of DPC based on crystal (from top to down), and (d) schematic of proposed assembly mode.

space group  $C 2/c$  had cell parameters of  $a=26.85 \text{ \AA}$ ,  $b=4.40 \text{ \AA}$ ,  $c=31.73 \text{ \AA}$ ,  $\alpha=90.00^\circ$ ,  $\beta=96.71^\circ$  and  $\gamma=90.00^\circ$  (Table S1). Interestingly, the ethanol interplayed with DPC by multiple H-bond, the distances of  $C-H\cdots O$  were 2.702, 2.783 and 2.796  $\text{\AA}$ . Moreover, the interaction of  $O-H\cdots N$  had a short distances of 2.153 and 2.657  $\text{\AA}$ . Besides, there were  $C-H\cdots O$  interactions and  $\pi-\pi$  stacking between DPC with the distances of 2.641 and 3.311  $\text{\AA}$ , respectively (Figure 3a). All of the above interactions ensured the formation of nanofibers and nanoribbons. In Figure 3b, adjacent DPC molecules arranged along the  $b$ -axis of the crystal to form single array, two such single arrays with same oriented molecules composed double array with a herringbone-like arrangement. XRD patterns further revealed the structures (Figure 3c). The characteristic reflection of DPC at  $2\theta=5.9^\circ$ ,  $d=14.9 \text{ \AA}$  (002),  $2\theta=11.9^\circ$ ,  $d=7.4 \text{ \AA}$  (004) and  $2\theta=21.2^\circ$ ,  $d=4.2 \text{ \AA}$  (600) assigned to the distances of ethanol and phenanthroline moiety which fitted well with crystal-based simulated XRD pattern (Figure 3a,c). Interestingly, the DPC/Cs possessed a similar characteristic reflection, with  $d=15.0 \text{ \AA}$  (002),  $d=7.5 \text{ \AA}$  (004) and  $d=4.1 \text{ \AA}$  (600). This hinted the similar structural mode with DPC, the larger distances indicated that the addition of CsCl altered the stacking of phenanthroline. This surprising result indicated that the  $\pi$ -stacking of phenanthroline moieties and H-bond between DPC and ethanol were important for the assembly of DPC and DPC/Cs. The binding of phenanthroline to  $Ni^{2+}$  and  $Ag^+$  broke the H-bond, resulted in the formation of amorphous structure of nanospheres and nanoparticles (Figure 3c). A reasonable assembly mode was illustrated in Figure 3d. However, the H-bonds

between DPC and ethanol were absent in solution although it existed in solid (Figure S19).

Electrochemistry is a useful tool for monitoring supramolecular self-aggregates.<sup>[13]</sup> To investigate the electrochemical property of assemblies, we recorded the cyclic voltammograms (CVs) in an ethanol/acetonitrile solution containing  $NBu_4PF_6$  (Figure 4a). The electrochemical curve showed

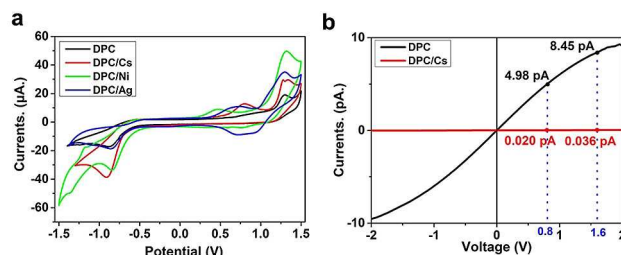


**Figure 4.** (a) Cyclic voltammograms of assemblies in ethanol/acetonitrile solution containing 0.10 M  $NBu_4PF_6$  (Sweep rate is  $100 \text{ mVs}^{-1}$  at  $25^\circ\text{C}$ ); (b) I-V curves of DPC and DPC/Cs.

a reduction wave at  $E=1.29 \text{ V}$  ( $18.78 \mu\text{A}$ ) and oxidation wave at  $E=-0.87 \text{ V}$  ( $17.00 \mu\text{A}$ ) for DPC. DPC/Cs displayed similar reduction wave at  $E=1.27 \text{ V}$  ( $29.27 \mu\text{A}$ ) and oxidation wave at  $E=-0.91 \text{ V}$  ( $-38.52 \mu\text{A}$ ), with additional reduction wave at  $E=0.79 \text{ V}$  ( $12.67 \mu\text{A}$ ). However, DPC/Ni gave a lower reduction wave at  $E=0.46 \text{ V}$  ( $8.89 \mu\text{A}$ ) and higher oxidation wave at  $E=-0.84 \text{ V}$  ( $-33.46 \mu\text{A}$ ). The DPC/Ni showed a reduction wave at

$E = 0.68$  V ( $10.78 \mu\text{A}$ ) and oxidation wave at  $E = -0.85$  V ( $-18.74 \mu\text{A}$ ) and  $E = 0.70$  V ( $-8.62 \mu\text{A}$ ). Obviously, the electrochemical property of assemblies had been altered by metals. The large size of DPC crystal and DPC/Cs nanoribbon spurred us to explore their conducting behaviour. DPC crystal wire was fixed on the two-terminal microscale gold electrode on glass base. The measured I–V characteristics of individual DPC at room temperature was displayed in Figure 4b. The nonlinear relationship suggested that the I–V behaviour of DPC obeys Ohm's law only at low applied voltage, and an intimately ohmic contact existed between the electrodes and crystal.<sup>[14]</sup> For DPC/Cs system, only 0.020 and 0.036 pA of current were detected at 0.8 and 1.6 V separately, while the current was 4.98 and 8.45 pA for DPC system. This could be attributed to the greater distance of phenanthroline in DPC/Cs system which lowered mobility of electron and hole.<sup>[15]</sup> The measurement of conducting behaviour for DPC/Ni and DPC/Ag was unavailable because their size (nanoscale) far below the requirement of 10  $\mu\text{m}$ .

In conclusion, the diphenanthroline crown ether could self-assemble into nanofibers, then transformed into nanoribbons, nanospheres and nanoparticles by the complexation of  $\text{Cs}^+$ ,  $\text{Ni}^{2+}$  and  $\text{Ag}^+$ . Crystal structure revealed the existence of  $\pi$ -stacking and H-bond between DPC and ethanol in solid. The strong ion-dipole interaction of  $\text{Ni}^{2+}$  or  $\text{Ag}^+$  with phenanthroline unit ensured the further tune. Moreover, the electrochemical property of assemblies had been altered by metals. Besides, the tiny extending of molecular distances in assembly resulted in significantly decreasing of conducting capability. This multilevel morphological manipulation enriched the methods to control and regulate the supramolecular assembly which had a potential application in material manufacturing.

CCDC 1884016 (DPC) contains the supplementary crystallographic data for this paper. These data can be obtained free of charge from The Cambridge Crystallographic Data Centre.

## Experimental Section Acknowledgements

This work was supported by NSFC (21432004, 21861132001, 21672113, 21772099 and 91527301).

## Conflict of Interest

The authors declare no conflict of interest.

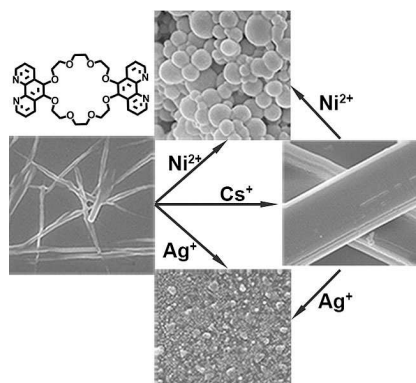
**Keywords:** crown ethers · morphological modulation · organic crystals · self-assembly · supramolecular chemistry

- [1] a) W. Jin, T. Fukushima, M. Niki, A. Kosaka, N. Ishii, T. Aida, *Proc. Natl. Acad. Sci. USA* **2005**, *102*, 10801–10806; b) P. A. Korevaar, S. J. George, A. J. Markvoort, M. M. Smulders, P. A. Hilbers, A. P. Schenning, T. F. De Greef, E. W. Meijer, *Nature* **2012**, *481*, 492–496; c) G. Mayer, A. Heckel, *Angew. Chem. Int. Ed. Engl.* **2006**, *45*, 4900–4921; d) Y. Yang, Y.-M. Zhang, Y. Zhang, X. Xu, Y. Liu, *Chem. Asian J.* **2015**, *10*, 84–90; e) Z. a. Li, S. Mukhopadhyay, S.-H. Jang, J.-L. Brédas, A. K. Y. Jen, *J. Am. Chem. Soc.* **2015**, *137*, 11920–11923; f) E. Y.-H. Hong, V. W.-W. Yam, *ACS Appl. Mater. Interfaces* **2017**, *9*, 2616–2624; g) X. Li, Y. Xie, B. Song, H.-L. Zhang, H. Chen, H. Cai, W. Liu, Y. Tang, *Angew. Chem. Int. Ed.* **2017**, *56*, 2689–2693; *Angew. Chem.* **2017**, *129*, 2733–2737; h) V. Montes-García, B. Gómez-González, D. Martínez-Solís, J. M. Taboada, N. Jiménez-Otero, J. de Uña-Álvarez, F. Obelleiro, L. García-Río, J. Pérez-Juste, I. Pastoriza-Santos, *ACS Appl. Mater. Interfaces* **2017**, *9*, 26372–26382; i) H. Xia, H. Fu, Y. Zhang, K.-C. Shih, Y. Ren, M. Anuganti, M.-P. Nieh, J. Cheng, Y. Lin, *J. Am. Chem. Soc.* **2017**, *139*, 11106–11116.
- [2] a) T. Fukino, H. Joo, Y. Hisada, M. Obana, H. Yamagishi, T. Hikima, M. Takata, N. Fujita, T. Aida, *Science* **2014**, *344*, 499–504; b) J. N. Smith, J. M. Hook, N. T. Lucas, *J. Am. Chem. Soc.* **2018**, *140*, 1131–1141; c) M. R. Cedano, D. K. Smith, *J. Org. Chem.* **2018**, *83*, 11595–11603.
- [3] a) S. Ogi, K. Sugiyasu, S. Manna, S. Samitsu, M. Takeuchi, *Nat. Chem.* **2014**, *6*, 188–195; b) S. Yagai, M. Usui, T. Seki, H. Murayama, Y. Kikkawa, S. Uemura, T. Karatsu, A. Kitamura, A. Asano, S. Seki, *J. Am. Chem. Soc.* **2012**, *134*, 7983–7994; c) K. Oohora, Y. Onuma, Y. Tanaka, A. Onoda, T. Hayashi, *Chem. Commun.* **2017**, *53*, 6879–6882; d) S. Li, R. Liu, D. Bekana, Y. Lai, J. Liu, *Nanoscale* **2018**, *10*, 20804–20812.
- [4] a) H.-L. Sun, Y. Chen, J. Zhao, Y. Liu, *Angew. Chem. Int. Ed.* **2015**, *54*, 9376–9380; *Angew. Chem.* **2015**, *127*, 9508–9512; b) Q. Si, Y. Feng, W. Yang, L. Fu, Q. Yan, L. Dong, P. Long, W. Feng, *ACS Appl. Mater. Interfaces* **2018**, *10*, 29909–29917; c) Z.-Z. Gao, J. Kan, Z. Tao, B. Bian, X. Xiao, *New J. Chem.* **2018**, *42*, 15420–15426; d) J. Chen, F. K.-C. Leung, M. C. A. Stuart, T. Kajitani, T. Fukushima, E. van der Giessen, B. L. Feringa, *Nat. Chem.* **2017**, *10*, 132; e) X. Li, J. Fei, Y. Xu, D. Li, T. Yuan, G. Li, C. Wang, J. Li, *Angew. Chem. Int. Ed.* **2018**, *57*, 1903–1907; *Angew. Chem.* **2018**, *130*, 1921–1925.
- [5] a) H.-L. Sun, Y. Chen, X. Han, Y. Liu, *Angew. Chem. Int. Ed.* **2017**, *56*, 7062–7065; *Angew. Chem.* **2017**, *129*, 7168–7171; b) W. Zhang, Y.-M. Zhang, S.-H. Li, Y.-L. Cui, J. Yu, Y. Liu, *Angew. Chem. Int. Ed.* **2016**, *55*, 11452–11456; *Angew. Chem.* **2016**, *128*, 11624–11628.
- [6] a) R. M. Izatt, R. E. Terry, D. P. Nelson, Y. Chan, D. J. Eatough, J. S. Bradshaw, L. D. Hansen, J. J. Christensen, *J. Am. Chem. Soc.* **1976**, *98*, 7626–7630; b) T. G. Levitskaia, J. C. Bryan, R. A. Sachleben, J. D. Lamb, B. A. Moyer, *J. Am. Chem. Soc.* **2000**, *122*, 554–562; c) E. Melnic, E. B. Coropceanu, A. Forni, E. Cariati, O. V. Kulikova, A. V. Siminel, V. C. Kravtsov, M. S. Fonari, *Cryst. Growth Des.* **2016**, *16*, 6275–6285.
- [7] J. C. Bryan, R. A. Sachleben, B. P. Hay, *Inorg. Chim. Acta.* **1999**, *290*, 86–94.
- [8] K. K. Bania, R. C. Deka, *J. Phys. Chem. C* **2011**, *115*, 9601–9607.
- [9] W. C. Vosburgh, G. R. Cooper, *J. Am. Chem. Soc.* **1941**, *63*, 437–442.
- [10] P. Yang, F. Cui, X.-J. Yang, B. Wu, *Cryst. Growth Des.* **2013**, *13*, 186–194.
- [11] J.-R. Su, D.-J. Xu, *Acta Crystallogr. Sect. E* **2005**, *61*, 1738–1740.
- [12] U. Velten, M. Rehahn, *Chem. Commun.* **1996**, 2639–2640.
- [13] a) P. L. Boulas, M. Gómez-Kaifer, L. Echegoyen, *Angew. Chem. Int. Ed.* **1998**, *37*, 216–247; *Angew. Chem.* **1998**, *110*, 226–258; b) G. Cooke, *Angew. Chem. Int. Ed.* **2003**, *42*, 4860–4870; *Angew. Chem.* **2003**, *115*, 5008–5018.
- [14] W. Zhu, R. Zheng, Y. Zhen, Z. Yu, H. Dong, H. Fu, Q. Shi, W. Hu, *J. Am. Chem. Soc.* **2015**, *137*, 11038–11046.
- [15] T. Wöhrle, I. Wurzbach, J. Kirres, A. Kostidou, N. Kapernaum, J. Litterscheidt, J. C. Haenle, P. Staffeld, A. Baro, F. Giesselmann, S. Laschat, *Chem. Rev.* **2016**, *116*, 1139–1241.

Manuscript received: January 7, 2019  
Revised manuscript received: January 9, 2019  
Accepted manuscript online: January 10, 2019  
Version of record online: ■■■, ■■■■

## COMMUNICATIONS

**Tunable nanoarchitectures** have been constructed from diphenanthro-24-crown-8 ether (DPC) and metal ions. Multiple H-bonds between DPC and ethanol were found to be vital for assembly and manipulation. Complexation with  $\text{Ni}^{\text{II}}$  and  $\text{Ag}^{\text{I}}$  ions alters the electrochemical properties of the assemblies.



Z.-Y. Zhang, Dr. Y. Chen, Dr. Y. Zhou,  
Prof. Dr. Y. Liu\*

1 – 6

**Tunable Supramolecular Nanoarchitectures Constructed by the Complexation of Diphenanthro-24-Crown-8/Cesium(I) with Nickel(II) and Silver(I) Ions**



#Supramolecular #nanoarchitectures made up of diphenanthro-24-crown-8/cesium(I) with nickel(II) and silver(I) ions, Yu Liu et al. #NankaiUniversity

Share your work on social media! ChemPlusChem has added Twitter as a means to promote your article. Twitter is an online microblogging service that enables its users to send and read short messages and media, known as tweets. Please check the pre-written tweet in the galley proofs for accuracy. If you, your team, or institution have a Twitter account, please include its handle @username. Please use hashtags only for the most important keywords, such as #catalysis, #nanoparticles, or #proteindesign. The ToC picture and a link to your article will be added automatically, so the tweet text must not exceed 250 characters. This tweet will be posted on the journal's Twitter account (follow us @ChemPlusChem) upon publication of your article in its final (possibly unpaginated) form. We recommend you to re-tweet it to alert more researchers about your publication, or to point it out to your institution's social media team.

#### ORCID (Open Researcher and Contributor ID)

Please check that the ORCID identifiers listed below are correct. We encourage all authors to provide an ORCID identifier for each coauthor. ORCID is a registry that provides researchers with a unique digital identifier. Some funding agencies recommend or even require the inclusion of ORCID IDs in all published articles, and authors should consult their funding agency guidelines for details. Registration is easy and free; for further information, see <http://orcid.org/>.

Dr. Yong Chen

Dr. Yan Zhou

Zhi-Yuan Zhang <http://orcid.org/0000-0001-9683-5034>

Prof. Dr. Yu Liu